Electronic Supplementary Material (ESI) for Organic & Biomolecular Chemistry.
This journal is © The Royal Society of Chemistry 2019

β-hairpin as peptidomimetics of phosphate-binding domains

I. L. Batalha[a,‡,*], I. Lychko[a,*], R. J. F. Branco[a], O. Iranzo[b] and A. C. A. Roque[a]

[a.] UCIBIO, Departamento de Química, Faculdade de Ciências e Tecnologia, Universidade Nova de Lisboa, Campus Caparica, 2829-516 Caparica, Portugal. E-mail: cecilia.roque@fct.unl.pt; Fax: +351 21 294 8550
[b.] Aix Marseille Univ, CNRS, Centrale Marseille, iSm2, Marseille, France. E-mail: olga.iranzo@univ-amu.fr
‡New address: Nanoscience Centre, Department of Engineering, University of Cambridge, 11 J.J. Thomson Avenue, Cambridge CB3 0FF, United Kingdom
* Authors contributed equally

Experimental

Chemical and Chromatographic material. All reagents and solvents used for synthesis, characterization and binding studies were of the highest purity available and the solvents were HPLC-gradient. Fmoc amino acid derivatives, the coupling reagents 2-(1H-benzotriazole-1-yl)-1,1,3,3-tetramethyluronium hexafluorophosphate (HBTU) and O-(7-azabenzotriazole-1-yl)-N,N,N',N'-tetramethyluronium hexafluorophosphate (HATU), as well as H-Gly-2-ClTrt and H-Glu(OtBu)-2-ClTrt resins were acquired from Novabiochem. 2-(N-Morpholino)ethanesulfonic acid (MES), 4-(2-hydroxyethyl)piperazine-1-ethanesulfonic acid (HEPES), 5,5'-dithiobis(2-nitrobenzoic acid) (Ellman's reagent), acetic anhydride, ammonium hydroxide solution, anisole, bicinchoninic acid kit for protein determination (BCA), diethyl ether, epichlorohydrin, ethanothiol, ethylenediaminetetraacetic acid (EDTA), ethylenediaminetetraacetic acid tetrasodium salt hydrate (EDTA-Na), iodoacetic anhydride, N-(3-dimethylaminopropyl)-N'-ethylcarbodiimide (EDC), N,N-diisopropylethylamine (DIEA), N-Hydroxysuccinimide (NHS), ninhydrin, phenol, piperidine, potassium cyanide, pyridine, sodium phosphate dibasic heptahydrate, sodium phosphate monobasic monohydrate thioanisole, trifluoroacetic acid (TFA), triisopropylsilane (TIS), tris(hydroxymethyl)aminomethane (TRIS), Tween 20 (Polysorbate 20) and β-mercaptoethanol were obtained from Sigma-Aldrich. Acetonitrile (ACN), bond-Breaker tris(2-carboxyethyl)phosphine (TCEP) solution, chloroform, dichloromethane (DCM), methanol (MeOH), N,N-dimethylformamide (DMF), and N-methyl-2-pyrrolidone (NMP) were obtained from Fisher Scientific. Ethanol, sodium chloride (NaCl), and sodium hydroxide (NaOH) were purchased from Panreac. 2-Propanol and L-cysteine were purchased from Roth and Acros Organic, respectively. Cyanine 5-maleimide (Cy5) was obtained from Lumiprobe. Nitrogen gas was supplied by Air Liquide. Gly-Ala-Ala-Tyr-Asp-Ile-Ser-Gln-Val-Phe-Pro-Phe-Ala-Lys (GK14), Gly-Ala-Ala-Tyr-Asp-Ile-pSer-Gln-Val-Phe- Pro-Phe-Ala-Lys (GK14-P), pTyr-Gly-Gly-Ile-Pro-Trp (YW6-P), Tyr-Gly-Gly-Ile-Pro-Trp (YW6), Tyr-Ala-Gly-pSer-pThr-Asp-Glu-Asn-pThr-Asp-Ser-Glu-Trp (YW13-P) and Tyr-Ala-Gly-Ser-Thr-Asp-Glu-Asn-Thr-Asp-Ser-Glu-Trp (YW13) peptides (p- is phosphorylated group) with N- and C- free terminals, were > 98% pure and were obtained from Genecust.

Sepharose™ CL-6B was acquired from GE Healthcare. Captiva 96-well 20µm filter plate with the respective duo seal 96-well Pl seal and Captiva 96-well plate cover were purchased from Agilent Technologies. Half-area UV-Star® 96-well microplates and 96-well transparent microplates were obtained from Greiner Bio-One and Sarstedt, respectively.

Methods

Full deprotection of peptides. Aliquots from peptides M0, M3 and M9 containing Cys residues, were dissolved in 2 mL of TFA/thioanisole/1,2-ethanedithiol/anisole (%v/v=90:5:3:2) and aliquot from peptide M9 with Glu at position 1 in 2 mL of TFA/water/TIS (%v/v=95:2.5:2.5) and stirred for 2 h under nitrogen gas. Resin was removed by filtration and the filtrate solution was reduced under a Nitrogen stream. Cold diethyl ether was added to the concentrated solution to precipitate the peptide which was subsequently washed several times with cold diethyl ether. Samples were analyzed by ESI-MS using an API-linear ion trap in positive ion mode. The following peaks were detected *(m/z):* linear M0 (MW=1028.4 Da) $[M+H]^{+}$- 1029.4, $[M+H+K]^{2+}$- 534.2, $[M+H+Na]^{2+}$- 526.2 and $[M+2H]^{2+}$- 515.2; linear M9 (MW = 1275.6 Da) $[M+2H]^{2+}$- 638.8 and $[M+3H]^{3+}$- 426.2; linear M3 (MW = 1329.7 Da) $[M+H]^{+}$- 1330.7, $[M+2H]^{2+}$- 665.9, $[M+H+K]^{2+}$- 684.8, $[M+2K+K]^{3+}$- 456.9; linear M9(Glu) (MW=1301 Da) $[M+H]^{+}$- 1302 and $[M+2H]^{2+}$- 652.

Table S1 - Peptidomimetic model sequences.

BRCT Model	Peptidomimetic Sequence
Template	Lys_1- Gly_2–Arg_3-Arg_4-Ile_5 -Arg_6 -Ile_7-$^{D}Pro_8$-$^{L}Pro_9$-Arg_{10}-Val_{11}-Arg_{12}-Thr_{13}-Arg_{14}
00	Met_1-Gly_2-$\mathbf{Gly_3}$-Gly_4-Gly_5 -Gly_6 -Gly_7-$^{D}Pro_8$-$^{L}Pro_9$-Gly_{10}-Val_{11}- $\mathbf{Gly_{12}}$-Thr_{13}- Gly_{14}
01	Arg_1-Gly_2-$\mathbf{Phe_3}$-Gly_4-Ile_5 -Gly_6 -Ile_7-$^{D}Pro_8$-$^{L}Pro_9$-Gly_{10}-Val_{11}-$\mathbf{Arg_{12}}$-Thr_{13}- Gly_{14}
02	Phe_1-Gly_2-$\mathbf{Arg_3}$- Gly_4-Ile_5 -Gly_6 -Ile_7-$^{D}Pro_8$-$^{L}Pro_9$-Gly_{10}-Val_{11}-$\mathbf{Arg_{12}}$-Thr_{13}- Gly_{14}
03	Arg_1-Gly_2-$\mathbf{Phe_3}$-Gly_4-Ile_5 -Gly_6 -Ile_7-$^{D}Pro_8$-$^{L}Pro_9$-$\mathbf{Arg_{10}}$-Val_{11}-Gly_{12}-Thr_{13}- Gly_{14}
04	Phe_1-Gly_2-$\mathbf{Arg_3}$- Gly_4-Ile_5 -Gly_6 -Ile_7-$^{D}Pro_8$-$^{L}Pro_9$-$\mathbf{Arg_{10}}$-Val_{11}-Gly_{12}-Thr_{13}- Gly_{14}
05	Arg_1-Gly_2-$\mathbf{Phe_3}$-Gly_4-Ile_5 -Gly_6 -$\mathbf{Arg_7}$-$^{D}Pro_8$-$^{L}Pro_9$-Gly_{10}-Val_{11}- Ile_{12}-Thr_{13}- Gly_{14}
06	Phe_1-Gly_2 -$\mathbf{Arg_3}$-Gly_4-Ile_5 -Gly_6-$\mathbf{Arg_7}$- $^{D}Pro_8$-$^{L}Pro_9$-Gly_{10}-Val_{11} -Ile_{12}-Thr_{13} -Gly_{14}
07	Met_1-Gly_2-$\mathbf{Phe_3}$-Gly_4-Ile_5 -Gly_6 -Ile_7-$^{D}Pro_8$-$^{L}Pro_9$-Gly_{10}-Val_{11}-$\mathbf{Arg_{12}}$-Thr_{13}- Gly_{14}
08	Met_1-Gly_2-$\mathbf{Phe_3}$-Gly_4-Ile_5- Gly_6- Ile_7- $^{D}Pro_8$-$^{L}Pro_9$-$\mathbf{Arg_{10}}$-Val_{11}-Gly_{12}-Thr_{13} - Gly_{14}
09	Met_1-Gly_2-$\mathbf{Phe_3}$-Gly_4-$\mathbf{Dap_5}$-Gly_6-$\mathbf{Dap_7}$-$^{D}Pro_8$-$^{L}Pro_9$-Gly_{10}-Val_{11}-$\mathbf{Arg_{12}}$-Thr_{13} -Gly_{14}
10	Met_1-Gly_2-$\mathbf{Phe_3}$-Gly_4-$\mathbf{Dab_5}$-Gly_6-$\mathbf{Dab_7}$-$^{D}Pro_8$-$^{L}Pro_9$-Gly_{10}-Val_{11}-$\mathbf{Arg_{12}}$-Thr_{13} -Gly_{14}
11	Met_1-Gly_2-$\mathbf{Phe_3}$-Gly_4-$\mathbf{Orn_5}$-Gly_6-$\mathbf{Orn_7}$ -$^{D}Pro_8$-$^{L}Pro_9$-Gly_{10}-Val_{11}-$\mathbf{Arg_{12}}$-Thr_{13} -Gly_{14}
12	Arg_1-Gly_2- Gly_3- Gly_4-Ile_5- Gly_6 -Ile_7- $^{D}Pro_8$-$^{L}Pro_9$-Gly_{10}-Val_{11}-$\mathbf{Arg_{12}}$-Thr_{13}-$\mathbf{Phe_{14}}$

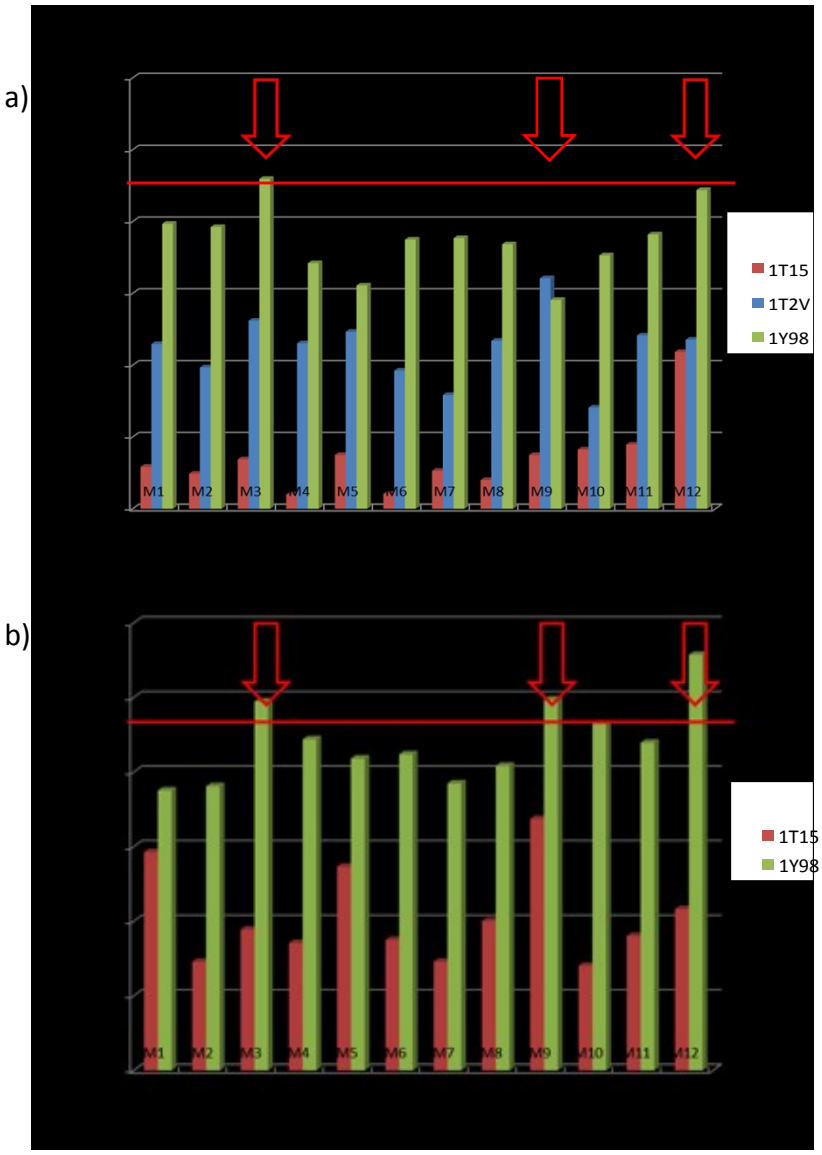

Figure S1 – a) Estimated free energy of binding from docking studies on the specific affinity of each structure-based designed model (M1-M12) to the phosphoserine peptides taken from BRCT-ligand complex structures 1T15, 1T2V and 1Y98. Beta-hairpin cyclic peptide models were considered as rigid docking targets, without any degree of flexibility on point-mutated side chains. **b)** Refinement of the estimated docking free energy of binding between M1 – M12 models and phosphoserine peptides taken from BRCT-ligand complex structures 1T15 and 1Y98. Point-mutated side chains on the beta-hairpin cyclic peptide models were allowed to have a maximum of 32 degrees of freedom in total. The red line indicates the threshold above -8.0 kcal/mol corresponding to an estimated K_i of 1.4 μM.

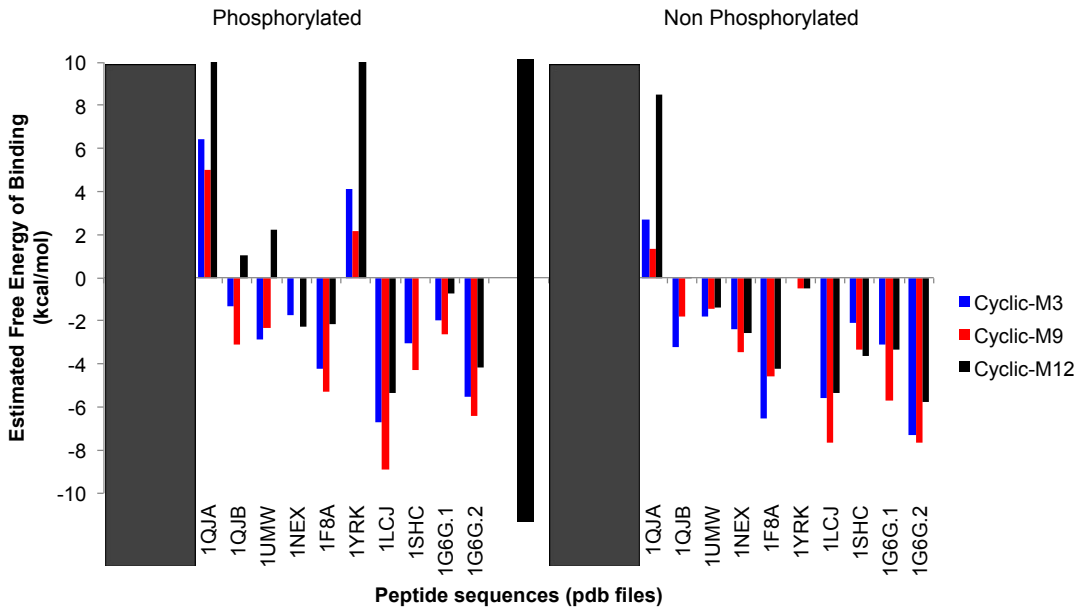

Figure S2 - Comparison of the estimated free energy of binding between phosphorylated and non-phosphorylated sequences against the best three structure-based design models M3, M9 and M12. Phosphopeptides on the x-axis are group by the corresponding specific binding domain sub-family, e.g. BRCT-specific binding domain marked within the grey box.

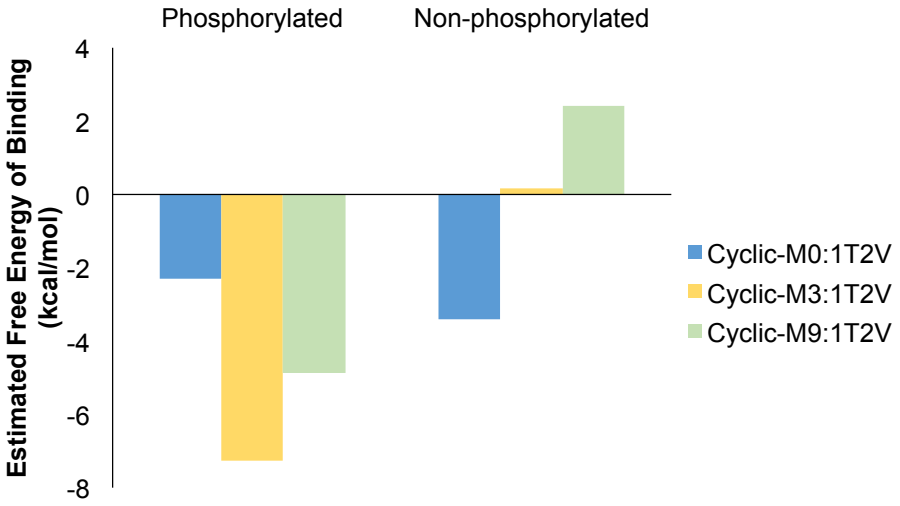

Figure S3 – Estimated free energy of binding obtained for the docking of phosphorylated and non-phosphorylated peptide GK14 with models M0, M3 and M9.

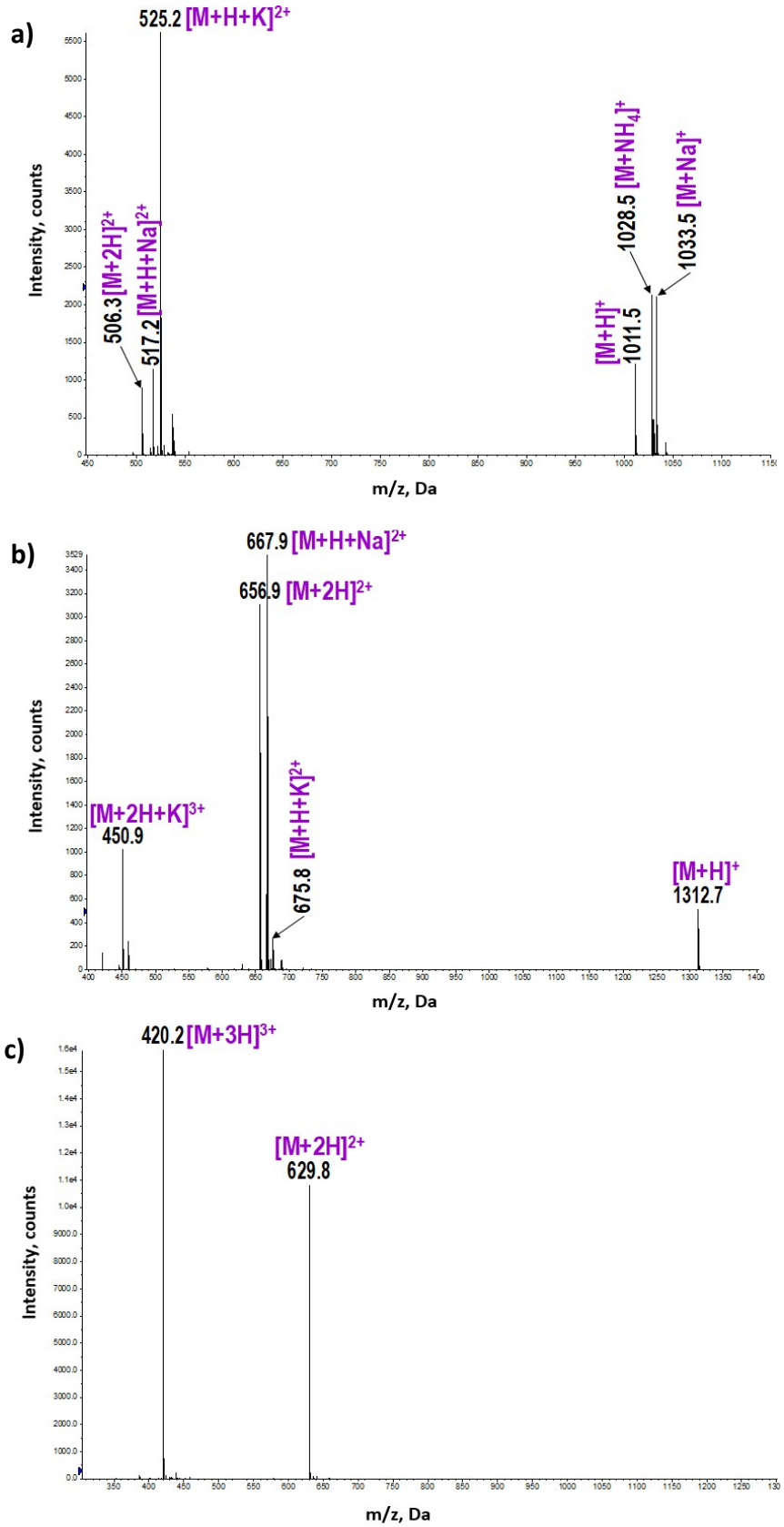

Figure S4 – ESI Mass spectra obtained in a positive ion mode for the purified cyclic peptidomimetics: **a)** Cyclic-M0, **b)** Cyclic-M3 and **c)** Cyclic-M9. M corresponds to the molecular weight of the respective cyclic peptide.

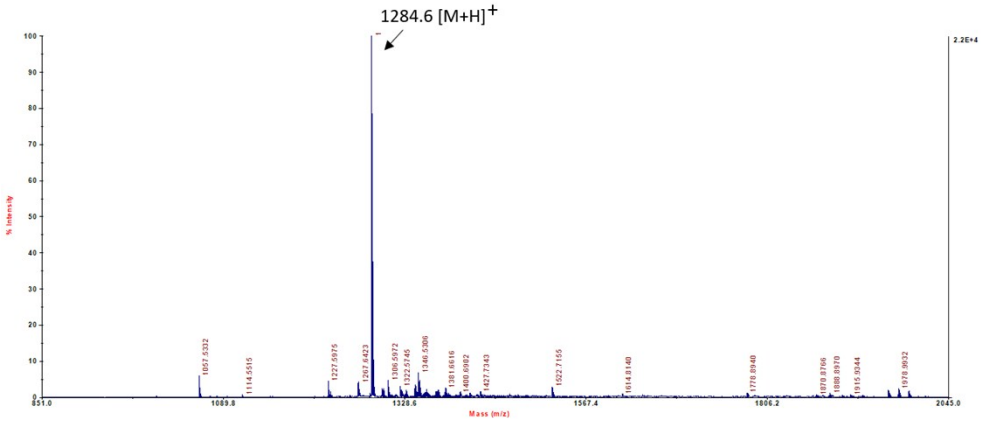

Figure S4 (Continuation) – ESI Mass spectra obtained in a positive ion mode for the purified cyclic peptidomimetics**: d)** Cyclic-M9(Glu). M corresponds to the molecular weight of the respective cyclic peptide.

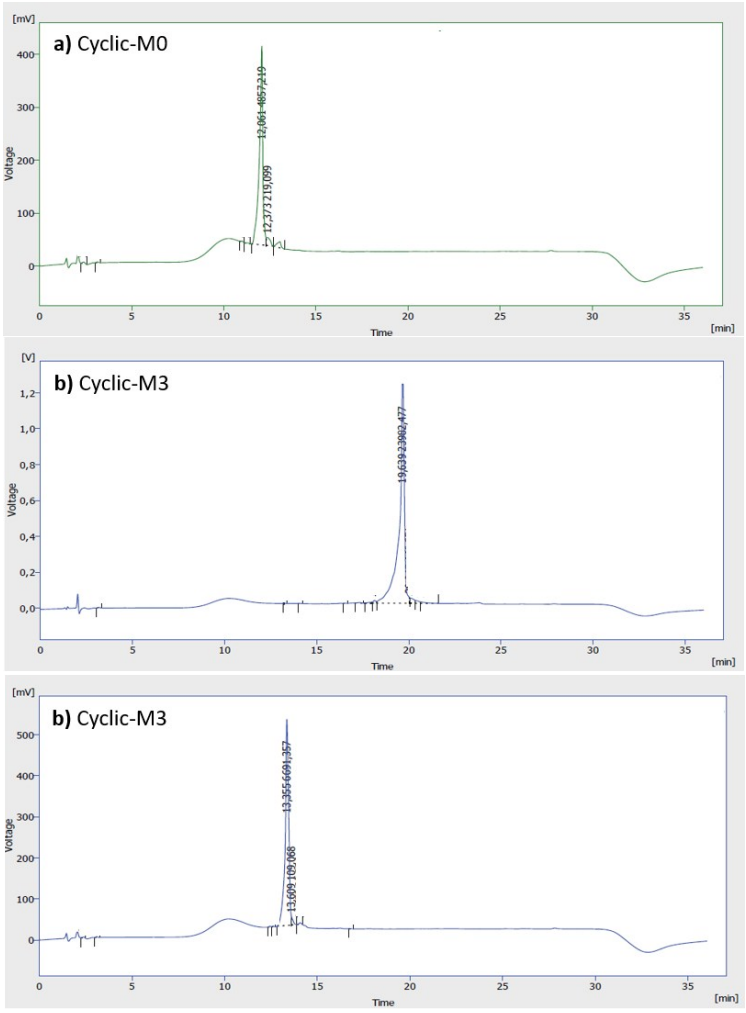

Figure S5 – HPLC traces of synthetized peptides: **a)** Cyclic-M0 **b)** Cyclic-M3 and **c)** Cyclic-M9. Linear gradient 5-45% of solvent B in 36 mim. solvent A (water/TFA, 99.9:0.1 v/v) and solvent B (ACN/water/TFA, 90:9.9:0.1 v/v), column Zorbax SB-C18 150 x 4.6 mm, detector UV/Vis 214 nm.

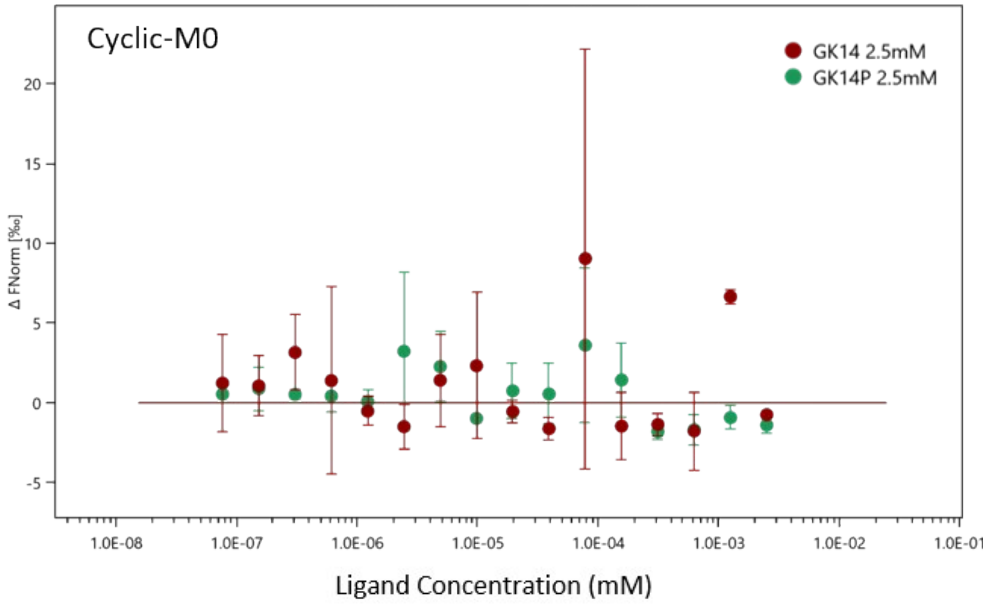

Figure S6 – Dose response curve fitted from MST assay. 10 nM of Cyclic-M0 were used in each assay with a serial dilution of GK14-P and GK14 (maximum concentration fixed at 2.5 mM).

Table S2 – Amino acid sequences of phosphorylated peptides comprising consensus sequences recognized by by FHA (YW13-P) and Src-like SH2 (YW6-P) domains, as well as their non-phosphorylated counterparts (YW13 and YW6). Phosphorylated residues are depicted in bold.

Peptide ID	Sequence
YW6-P	**pY**-G-G-I-P-W
YW6	Y-G-G-I-P-W
YW13-P	Y-A-G-**pS**-**pT**-D-E-N-**pT**-D-S-E-W
YW13	Y-A-G-S-T-D-E-N-T-D-S-E-W

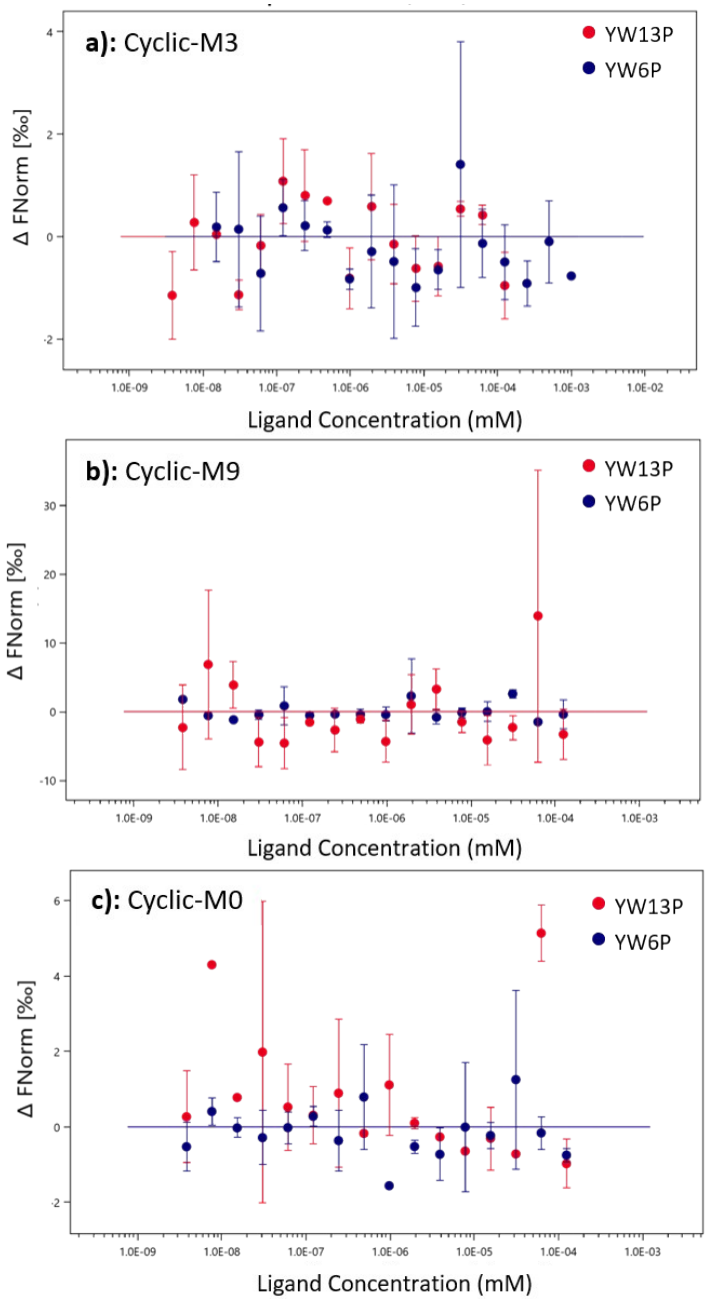

Figure S7 – Dose response curve fitted from MST assay. 10 nM of labeled cyclic peptides were used in each assay with a variation of YW13-P and YW6-P concentrations (maximum fixed at 0.125 mM). **a)** Cyclic-M3; **b)** Cyclic-M9; and **c)** Cyclic-M0

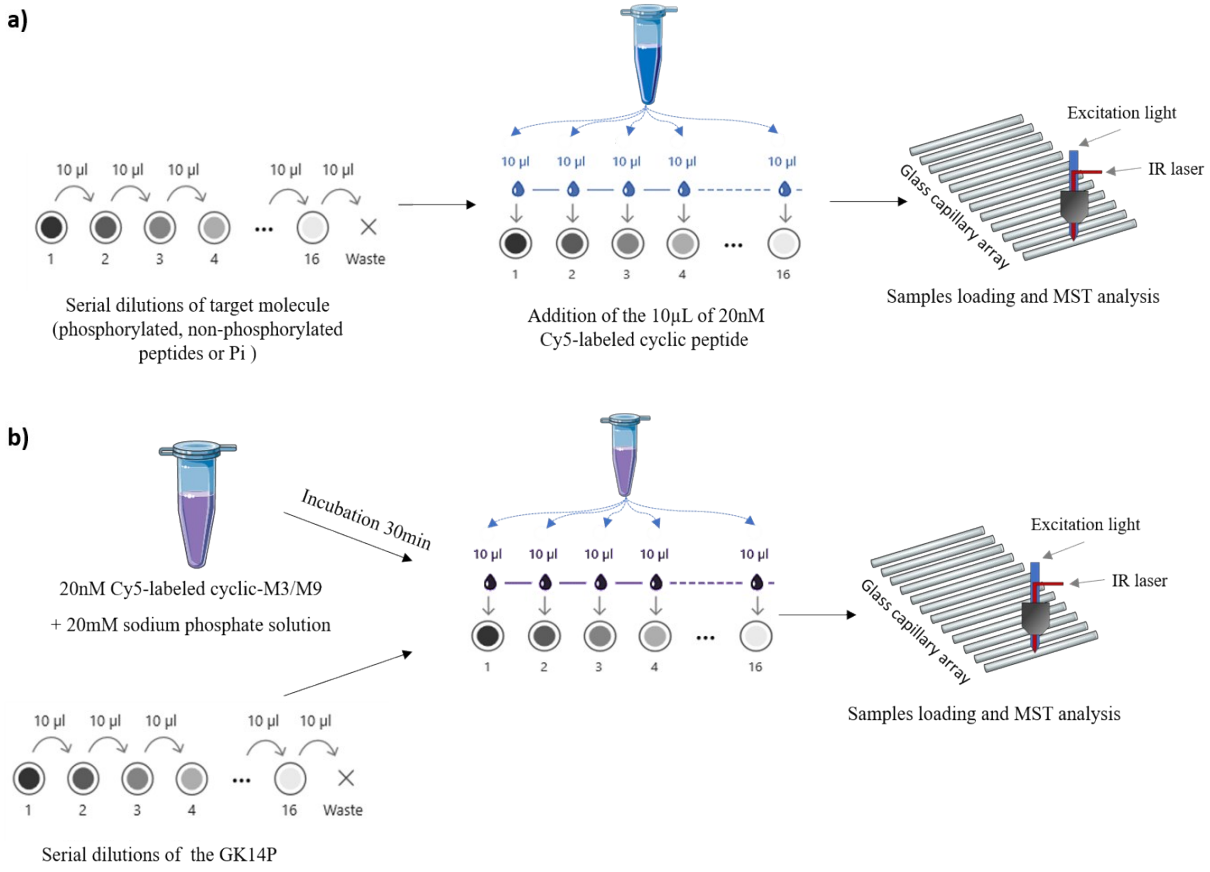

Figure S8 – Schematic overview of the samples preparation for **a)** standard MST experiment and **b)** competition experiment.

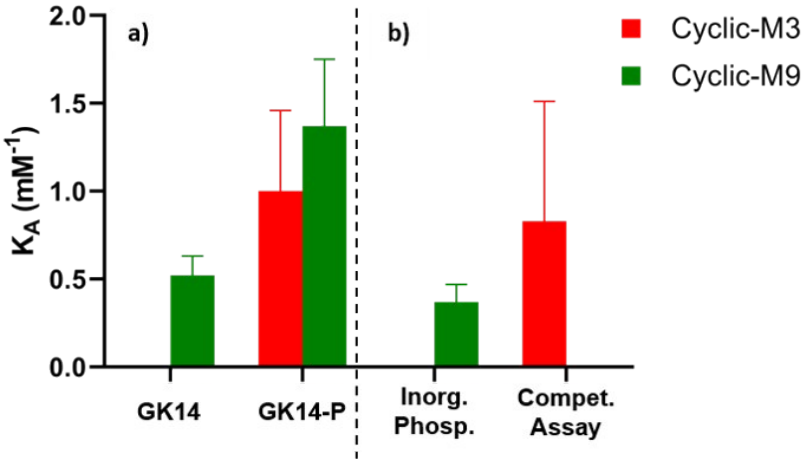

Figure S9 – Overview of the K_A (mM^{-1}) calculated from the deduced K_D values from the MST binding assays: **a)** assays with GK14-P, GK14; **b)** assays with Pi and competitive assay. Cyclic-M9 binds the Pi with K_A = 0.37 mM^{-1} and did not interact with GK14-P in the presence of Pi. Cyclic-M3 did not form a complex with Pi, however the competitive results were inconclusive.

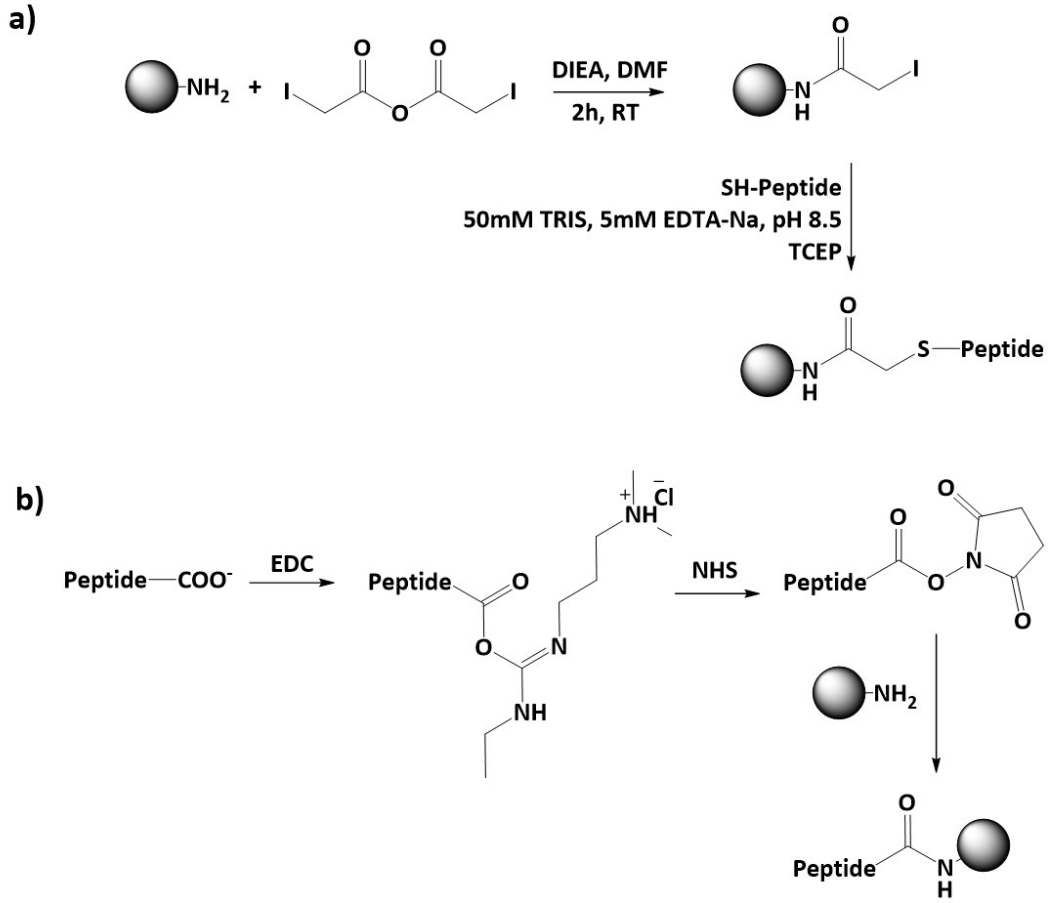

Figure S10 – a) Strategy for the immobilization of peptides through Cys residue. Aminated agarose reacts with iodoacetic anhydride to yield iodoacetylated agarose, which in turn reacts with peptides through their Cys sulfydryl groups. **b)** Immobilization of peptides through their carboxylic groups onto aminated agarose. Activation of carboxylic groups of peptides with EDC and NHS yields an amine-reactive ester, which reacts with aminated agarose at pH 7.